

Theoretical Consideration on Elastic Deformations of Aluminum  
by Pseudopotential Method\*

By Masafumi SENOO\*\*, Ikuya FUJISHIRO\*\*\*  
and Motohisa HIRANO\*\*\*\*

To discuss the elastic properties of aluminum, the variations of the crystal energy at 0K with the (100) lattice deformations are evaluated by means of the pseudopotential methods based on the model potential proposed by the authors previously. A distinction is made between the mechanical behavior of a face centered cubic (fcc) lattice in (100) loading (i.e. transverse stresses are zero) and in (100) deformation (i.e. transverse strains are zero). The fcc-bcc transitions and the elastic instabilities associated with the deformations are briefly discussed. Some elastic constants of aluminum at 0K are calculated. The stress-strain relations for large elastic strains up to the theoretical tensile strength are presented.

Key Words: Metallic Materials, Elasticity, Aluminum, Elastic Constants, Pseudopotential Method, Crystal Energy

### 1. Introduction

An elastic constant of solid materials is one of the most basic properties of mechanical behaviors. It is generally known that in principle it has a certain dependence on pressures and temperatures, and it is changed by machining such as rolling and drawing or by heat-treatments such as quenching and annealing<sup>(1)</sup>. Though elastic deformations on crystals are usually restricted to a very small strain, Milstein<sup>(2)</sup> has pointed out that any non-linearity of the stress-strain relations must be taken into account even under the elastic limit in the cases of the following conditions of deformations, because of the exceedingly large strain.

- (1) High-speed deformations as a shock loading, a martensite transformation and a generation of deformation twins.
- (2) Localized deformations near micro-crack-tip or other stress concentrations.
- (3) Deformations of perfect crystals as

whiskers.

To predict the variations of elastic constants with such various environments and conditions, the atomistic considerations on the elastic deformations of crystals are supposed to be one of the effective methods. So far, an interatomic force of the pairpotential such as Morse potential, whose parameters are usually determined by the elastic constants on a standard condition, has been often assumed for such calculations<sup>(2)(3)</sup>.

On the other hand, we can obtain thermodynamically the stresses induced by the elastic deformations of crystals (i.e. the homogenous deformation of crystal lattice), if the internal energy of crystals is evaluated as a function of the atomic configurations. The pseudopotential method has progressed rapidly in recent years. It has been successfully applied to calculate the properties of simple metals (of which the ion-core is comparatively small and the Fermi surface is nearly sphere, i.e. the electronic structure is close to that of free electrons)<sup>(4)(5)</sup>. However, some difficult points were recognized in the calculations of properties with variations of the crystal volume. The authors have proposed new model potentials which were successfully used for the calculations even in the case of very large volume change, and determined the pressure-volume relations of aluminum and other metals from these potentials<sup>(6)(7)</sup>. These calculated values fairly well agreed

\* Received 25th May, 1983.

\*\* Associate Professor, School of Engineering, Nagoya University, (Furou-cho, Chikusa-ku, Nagoya, Japan).

\*\*\* Professor, Mie University, (Kamihama-cho, Tsu, Japan).

\*\*\*\* Researcher, Musashino Electrical Communication, NTT, (Midori-cho, Musashino, Tokyo, Japan).

with the experimental values.

In the present paper, the elastic deformations of the aluminum single crystal at OK of temperature are theoretically investigated by making use of the model potential proposed by the authors previously. This is a basic step to prediction of the above-mentioned variations of the elastic constants. The variations of the crystal energy with the monoaxially homogenous deformations in the perpendicular direction to the (100) lattice plane of the crystal are evaluated by the pseudopotential method. The calculations are carried out under the conditions of two kinds of deformation modes; the monoaxial strain deformation in which the transverse strains are zero and the monoaxial stress deformation in which the transverse stresses are zero. Thus the elastic constants of  $C_{11}$ ,  $C_{12}$ , Young's modulus and Poisson's ratio are obtained, and are compared with some existing experimental values. The stress-strain relations under large deformations are also calculated to evaluate the variations of the elastic constants with strains and to consider the ideal fracture strength.

The face centered cubic lattice (fcc) such as aluminum is equivalent to the body centered tetragonal lattice with stretched crystal axis in the [100] direction (bct of  $\sqrt{2}$  in axial ratio)(c.f. Fig.1). Hence discussion is also made whether any elastic unstable caused by the fcc-bcc transformation under the monoaxial deformations appears or not.

## 2. Theory and Method of Calculations

### 2.1 Evaluation of the crystal energy

Following the pseudopotential method formulated by Harrison<sup>(4)</sup> and Heine<sup>(5)</sup>, the total energy of crystal  $U_t$  is, taking account of up to the second perturbation term, given by

$$U_t = U_{eg} + U_0 + U_{bs} + U_{es} \dots\dots\dots(1)$$

where  $U_{eg}$  is the energy of conduction electron gas,  $U_0$  the average value of the electron-ion interaction energy,  $U_{bs}$  the band structure energy, and  $U_{es}$  the electrostatic energy of ions immersed in conduction electron gas. The method of calculation of these terms besides  $U_{es}$  is the same as that in previous papers<sup>(6)(7)</sup>. Hence the formalisms to calculate the energy per atom with the atomic volume  $\Omega$  are briefly interpreted as follows. The numerical calculations in the present study were carried out in the atomic units having

$$\hbar = 2m = e^2/2 = 4\pi\epsilon_0 = 1 \dots\dots\dots(2)$$

where  $\hbar = h/2\pi$ ,  $h$  is Planck's constant,

$m$  the electron mass,  $e$  the electronic charge, and  $\epsilon$  the permittivity of free space, and then the final results were transformed into SI units.

The model potential which is used as the potential of the ion core to the conduction electron in crystals is

$$W^{ion}(r) = -A \quad \text{for } r \leq R_M$$

$$W^{ion}(r) = -\frac{Ze^2}{4\pi\epsilon_0 r} \quad \text{for } r > R_M$$

.....(3)

where the potential depth  $A$  and the radius  $R_M$  are parameters,  $z$  is the valence, i.e.  $z=3$  in aluminum, and  $r$  is a distance in radial direction. The potential parameters  $A$  and  $R_M$  are

$$A = 3.9005 \times 10^{-18} \text{ J}$$

$$R_M = 7.1599 \times 10^{-11} \text{ m} \dots\dots\dots(4)$$

as have been determined in the previous paper<sup>(7)</sup>.

The first term of Eq.(1) is written as

$$U_{eg} = Z \left( \frac{3\hbar^2 k_f^2}{10m} - \frac{3e^2 k_f}{16\pi^2 \epsilon_0} + U_{cor} \right) \dots\dots\dots(5)$$

$$k_f = (3\pi^2 Z/\Omega)^{1/3} \dots\dots\dots(6)$$

by using the Fermi wave number  $k_f$ . The first term of Eq.(5) is the kinetic energy of the conduction electrons, and the second term the exchange energy. The third term is the correlation energy,

$$U_{cor} = -0.115 + 0.031 \ln r_s \dots\dots\dots(7)$$

in use of the atomic units, which was proposed by Nozieres and Pines<sup>(8)</sup> in use of the atomic units.  $r_s$  is the density parameter of the conduction electrons,

$$r_s = (3\Omega/4\pi Z)^{1/3} \dots\dots\dots(8)$$

The second term of Eq.(1),  $U_0$ , is written as

$$U_0 = \frac{3Z^2 e^2}{8\pi\epsilon_0 R_a} \left( \frac{R_M}{R_a} \right)^2 - AZ \left( \frac{R_M}{R_a} \right)^3 \dots\dots\dots(9)$$

by using the potential parameters  $A$  and  $R_M$ .  $R_a$  is the radius of Wigner-Seitz cell given by

$$R_a = (3\Omega/4\pi)^{1/3} \dots\dots\dots(10)$$

As shown in Eqs.(1) ~ (5),  $U_{eg}$  and  $U_0$  are independent of the atomic configuration

$$U_{bs} = \sum_q |S(q)|^2 \{ W^{ion}(q)/\epsilon(q) \}^2$$

$$\times \chi(q)\epsilon(q) \dots\dots\dots(11)$$

by using the reciprocal lattice vector of the crystal,  $q$  (with its absolute value  $q$ ), where  $W^{ion}(q)$  is the Fourier transform of the potential  $W^{ion}(r)$  in Eq. (2),  $\chi(q)$  the perturbation characteristic,  $\epsilon(q)$  the dielectric function of conduction electrons, and  $S(q)$  is the crystal structure factor.

Now when the atomic sites are  $R_j$  and the atomic number is  $N$  in the crystal unit lattice, we have

$$S(q) = \frac{1}{N} \sum_{j=1}^N \exp(-iqR_j) \dots\dots\dots(12)$$

$$q = m_1 q_1 + m_2 q_2 + m_3 q_3 \dots\dots\dots(13)$$

where  $q_1$ ,  $q_2$  and  $q_3$  are unit vectors of the reciprocal lattice, and  $m_1$ ,  $m_2$  and  $m_3$  are arbitrary integers. And we have

$$W^{ion}(q) = -\frac{4\pi A}{\Omega q^3} \{ \sin(qR_M) - qR_M \times \cos(qR_M) \} - \frac{Ze^2}{\epsilon_0 \Omega q^2} \cos(qR_M) \dots\dots\dots(14)$$

$$\epsilon(q) = 1 - \frac{2e^2}{\epsilon_0 \Omega q^2} \{ 1 - f(q) \} \chi(q) \dots\dots\dots(15)$$

$$\chi(q) = -\frac{3Zm}{2h^2 k_f^2} \left( \frac{1}{2} + \frac{4k_f^2 - q^2}{8qk_f} \ln \left| \frac{q + 2k_f}{q - 2k_f} \right| \right) \dots\dots\dots(16)$$

As the correction function  $f(q)$  in Eq. (15), we take

$$f(q) = \frac{q^2}{2(q^2 + k_f^2 + 2k_f/\pi)} \dots\dots\dots(17)$$

in the atomic units, which was proposed by Sham<sup>(9)</sup> in atomic units.  $\Sigma'$  in Eq. (11) means the reciprocal lattice summation besides  $q=0$ . Thus  $U_{bs}$  depends not only on the atomic volume but also on the atomic configurations through the crystal structure factor  $S(q)$ .  $U_{bs}$  is therefore important in evaluating the variations of the internal energy with the monoaxial deformations. The right side in Eq. (11), however, converged rapidly with  $q$ , and the reciprocal lattice vectors were summed for 722 points in the range of  $q < 8k_f$  in the present calculation.

2. 2 Evaluation of the electrostatic energy

The final term of Eq. (1),  $U_{es}$ , which is the electrostatic energy of ions configured and immersed in the conduction electron gas, was generally given by Harrison<sup>(4)</sup> as

$$U_{es} = \frac{Z^2 e^2}{8\pi\epsilon_0} \lim_{\eta \rightarrow \infty} \left\{ \frac{4\pi}{\Omega} \sum_q |S(q)|^2 \times \frac{\exp(-q^2/4\eta)}{q^2} - \frac{2\sqrt{\eta}}{\sqrt{\pi}} \right\} \dots\dots\dots(18)$$

where  $\eta$  is a convergence factor. However, the convergence of this reciprocal lattice sum was so slow, that it was insufficient to take sum of even 9000 points. In the case of the previous calculations of the  $P-V$  relations on which the relative configuration of atoms was invariable and only the atomic volume was changed, it was possible to represent the dependence on the crystal structure by the Ewald coefficient  $\alpha$ . And

Eq. (18) was written as

$$U_{es} = \frac{\alpha Z^2 e^2}{8\pi\epsilon_0 R_a} \dots\dots\dots(19)$$

The Ewald coefficients for the face centered cubic (fcc) and the body centered cubic (bcc) structure were calculated by Sholl<sup>(10)</sup>, respectively, as follows

$$\left. \begin{aligned} \alpha^{fcc} &= -1.79175 \\ \alpha^{bcc} &= -1.79186 \end{aligned} \right\} \dots\dots\dots(20)$$

The calculated values of  $\alpha$  when the structure is transformed into face centered tetragonal (fct) by the monoaxial deformations have not been reported yet. A method to evaluate  $\alpha$  with the rapid convergence, however, has been proposed by Harrison<sup>(4)</sup>, when the axial ratio  $c/a$  is changed in a hexagonal closed pack (hcp) structure. He introduced lines parallel to  $c$ -axis through the reciprocal points in the reciprocal lattice space, and calculated the sum along the line and then the sum of the contribution by each line, in place of the sum for the whole reciprocal lattice vector  $q$ . In the present calculations, the variations of the electrostatic energy with the monoaxial deformations in the fcc structure are evaluated by means of this method. The Ewald coefficient for the fct,  $\alpha^{fct}$ , is finally written as a function of the axial ratio  $x (= a_1/a_2)$  by

$$\alpha^{fct} = \left( \frac{3\pi^2 x}{2} \right)^{1/3} \left\{ A + \frac{x}{6} + \frac{2}{\pi} \sum_{m_t} \mu(m_t) \right\} \dots\dots(21)$$

where  $\mu(m_t)$  is the contribution from the line of  $m_t = \sqrt{m_1^2 + m_2^2}$ . An arbitrary constant  $A$  was determined such that it agree with  $\alpha^{fct}$  at  $x=1$  (i. e. fcc). As the summation by  $m_t$  in Eq. (21) converged very rapidly, we could obtain the sufficient results from summing up to about 50 lines. The results are shown in Table 1 with that for bct. As shown in Fig. 1, the fcc lattice is equivalent to the bct lattice with the axial ratio  $a_1/a_2 = \sqrt{2}$ , while the bcc lattice is equivalent to the fct lattice with the axial ratio  $a_1/a_2 = 1/\sqrt{2}$ .

Table 1. Variations of Ewald coefficient with the axial ratio  $a_1/a_2$ .

$a_1/a_2$	$\alpha^{fct}$	$\alpha^{bcc}$
0.5	-1.77833	-1.68877
0.6	-1.79008	-1.75018
0.7	-1.79186	-1.77717
0.8	-1.79164	-1.78723
0.9	-1.79161	-1.79127
1.0	-1.79175	-1.79186
1.1	-1.79134	-1.79170
1.2	-1.78959	-1.79157
1.3	-1.78585	-1.79164
1.4	-1.77975	-1.79175
1.5	-1.77096	-1.79162

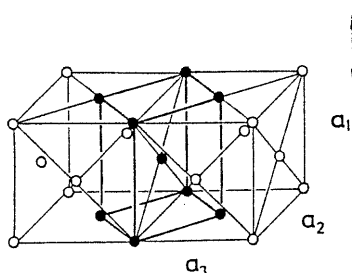


Fig. 1. The relation of the face centered cubic to the body centered tetragonal (in the case of  $c$ -axis parallel to the loading axis  $a_1$ ).

Therefore, the values of  $\alpha^{fct}$  at  $a_1/a_2 = 1/\sqrt{2}$  and  $\alpha^{bct}$  at  $a_1/a_2 = \sqrt{2}$  in Table 1 are in agreement with the value of  $\alpha^{fcc}$  and  $\alpha^{fcc}$ , respectively. They each correspond to the double minimum values.

### 2. 3 Definition and method of calculation of deformation modes

The variations of the crystal energy with the homogenous deformations in the  $\langle 100 \rangle$ -direction of the single crystal were evaluated in the present study. The calculations were carried out in two kinds of the deformation modes as follows: in the monoaxial strain-deformation (denoted by (100) deformation), the unit lattice  $a_1$  with unit vectors,  $a_1$ ,  $a_2$ ,  $a_3$ , shown in Fig. 1, was varied under the condition of  $a_2 = a_3 = \text{constant}$ ; in the monoaxial stress-deformation (denoted by (100) loading), after the unit lattice  $a_1$  was varied to have a nominal strain  $\lambda_1$ , the value of  $a_2 = a_3$  was adjusted to minimize the crystal energy  $U_t$ . The force applied to the (100)-plane of the unit lattice was calculated differentiating the crystal energy per unit lattice  $4U_t$  with respect to  $a_1$ . Then, the true stress was obtained from the force divided by the cross section of the unit lattice in both cases.

The elastic constants are determined by differentiating numerically the true stress

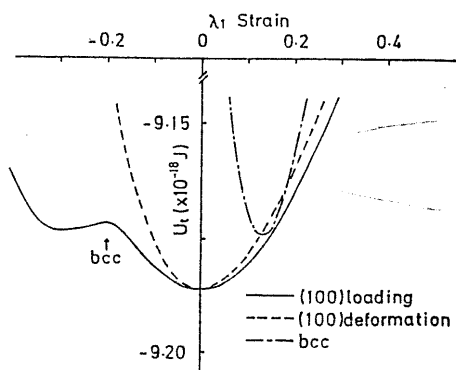


Fig. 2. Variations of the crystal energy with strain.

with respect to the true strain. For the elastic constants after some finite deformations of the nominal strain  $\lambda_1$ , we have taken differential coefficients with respect to the micro-strains ( $10^{-4}$  in step) normalized by  $\lambda_1$ . So these values are infinite strain elastic constants under the nominal strain  $\lambda_1$ . The numerical calculations have been carried out all to the double precision FORTRAN.

## 3. Calculated Results and Discussion

### 3.1 Variations of crystal energy and structure transformation

The variations of the crystal energy  $U_t$  with the nominal strain  $\lambda_1$  in the  $\langle 100 \rangle$  direction are shown in Fig. 2. In the (100) deformation mode the energy has varied monotonously as the anharmonic interplanar potential, no anomalous behavior was seen in the variations even at the point of the strain  $\lambda_1 = -0.293$  at which the crystal should be transformed into the bcc structure by the compressive deformation. The reason was supposed to be that the dependence of the crystal energy on the structure is hidden, because the Fermi energy is increased rapidly by the volumetric contraction in the compressive deformation. On the other hand, in the (100)-loading mode, a fall of the energy accompanied by the bcc structure transformation is clearly seen in the compressive deformation. At the strain  $\lambda_1 = -0.20$  where the bcc structure itself ( $a_1/a_2 = 1/\sqrt{2}$ ) appears, however,  $U_t$  shows maximum value, and shows minimum value at  $\lambda_1 = -0.29$ . The stable bcc structure is, therefore, not to be seen. It is considered that the crystal becomes unstable in elasticity for the compression at  $\lambda_1 = -0.11$  and over at which a point of inflection appears.

Recently in the pair-potential calculation for nickel and copper etc, Milstein<sup>(2) (1)</sup> has pointed out that a bifurcation of deformation mode in the stress-strain relation might possibly take place, because of the elastic instability accompanied with fcc-bcc transformation even in the tensile deforma-

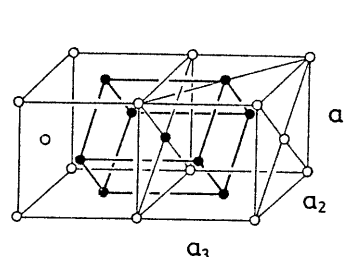


Fig. 3. fcc and bct.

tion. The crystal lattices are shown again in Fig.3. When  $a_1$  is deformed in tension and if  $a_2$  spreads and  $a_3$  shrinks, the crystal might be possibly transformed to the bcc structure. Straightforward discussions on such deformation mode are not to be done in the present calculations, for  $a_2$  and  $a_3$  could not be independently varied as mentioned in Sec.2.2. Therefore, postulating that the bcc structure appeared when the crystal lattice was deformed to stretch  $\lambda_1$ , calculations were carried out; i.e.  $U_t$  for a deformation mode with a restriction of  $a_1 = a_2 = a_3 / \sqrt{2}$  was evaluated. The results are shown in Fig.2. as the bcc mode. In this bcc mode  $U_t$  falls so rapidly near strain of  $\lambda_1 = 0.15$ , and is so close to the loading mode that the bcc structure might appear. Although bcc structure itself does not appear in the present calculations, it is reasonable speculated that the bifurcation on the tensile deformation pointed out by Milstein might take place.

3.2 Stress-strain relations and ideal fracture strength

The true stress  $\sigma_1$  is plotted against the nominal strain  $\lambda_1$  in Fig.4. In the (100)-deformation mode the maximum stress i.e. the ideal fracture strength  $\sigma_1^f = 17.4$  GPa is attained at  $\lambda_1 = 0.42$ . Examples of the stress-strain relation leading to fracture which are calculated based on such electron theory, have seldom been reported for aluminum. For copper, a calculation by using an augmented plane wave (APW) approximation is reported by Esposito<sup>(2)</sup>, where the

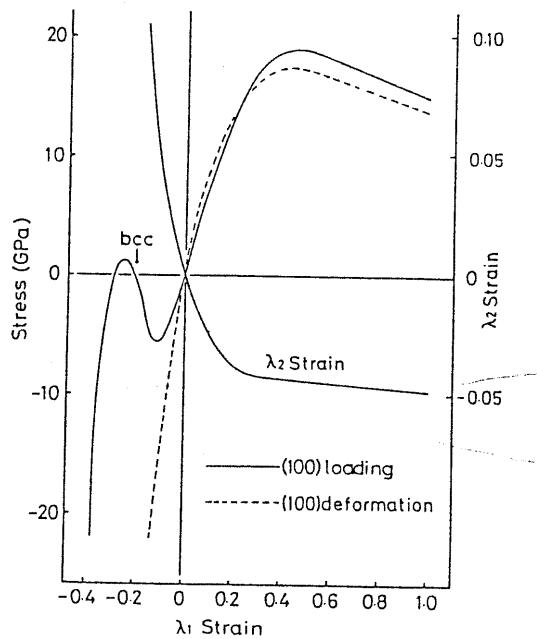


Fig.4. Stress-strain curves.

values of the fracture strain  $\lambda_1^f = 0.55$  and the fracture stress  $\sigma_1^f = 32$  GPa are obtained. On the other hand, in the (100)-loading mode the maximum true stress is  $\sigma_1^f = 19.0$  GPa at  $\lambda_1^f = 0.45$ .

In discussing the ideal fracture strength, an interplanar stress of crystals is sometimes approximately represented by a sine curve

$$\sigma = \sigma \left( \sin \left( \frac{\pi}{2} \frac{\lambda_1}{\lambda_1^f} \right) \right) \dots \dots \dots (22)$$

Applying the results of the present calculation to this equation, the stress-strain relation fits within the accuracy of a few percent. For example, substituting  $\sigma_1^f = 19.0$  GPa and  $\lambda_1^f = 0.45$ , the value of 68.3 GPa has been obtained as the initial slope of Eq.(22). This is in good agreement with Young's modulus  $E = 68.8$  GPa mentioned in the next section. In the compressive deformation over the unstable point at  $\lambda_1 = -0.11$  in the loading mode, the crystal should be assumed to have bcc structure with stress free at  $\lambda_1 = -0.20$ . But the stable bcc structure never appears because the stress-strain curve has negative slope at this point.

Although such large elastic deformations in aluminum are not realized usually experimentally, the calculated stress-strain relation may be supposedly useful, when stresses near crack tip or dislocation core is studied by a computer simulation etc. The calculated values are shown in Table 2. The stress-strain curve on the loading mode is convex downward near  $\lambda_1 = 0$ , and the stretch in  $\lambda_1$  is associated with a decrease in the transverse stretch  $\lambda_2$ , when  $\lambda_1 = 0.2$  and over,  $\lambda_2$  almost constant, i.e.,  $\lambda_2 \approx -0.04$ . These features show the same tendency shown in the calculated results with other materials by Milstein<sup>(2)(4)</sup>.

As the logarithmic term in Eq.(16) of  $\chi(\varphi)$  diverges at  $\varphi = 2k_f$ , we have used a limit value as  $\chi(\varphi)$  at this point.

Table 2. Calculated values of stress-strain relations.

Nominal Strain $\lambda_1$	Deformation Stress [GPa]	Loading Stress [GPa]	Loading Strain $\lambda_2$
-0.06	-7.82	-3.62	0.025
-0.04	-4.95	-2.49	0.016
-0.02	-2.35	-1.29	0.008
0.00	0.00	0.00	0.000
0.02	2.12	1.37	-0.007
0.04	4.03	2.80	-0.013
0.06	5.75	4.26	-0.018
0.08	7.29	5.71	-0.022
0.10	8.67	7.12	-0.026
0.20	13.56	13.16	-0.038
0.30	16.21	17.05	-0.043
0.40	17.41	18.82	-0.043
0.50	17.26	18.52	-0.045

Although the energy is correctly evaluated by such a method, its derivative diverges again. When the reciprocal lattice point  $q = 2k_f$  appears by chance during the deformations, therefore, it is impossible to obtain the details of the stress-strain relation near this point. This problem is left for further investigation. In the present calculation, as this point appeared near  $\lambda_1 = -0.11$  in the loading mode, the curve in Fig.4 was smoothly written near the point.

### 3.3 Elastic constants

The calculated elastic constants,  $C_{11}$  and  $C_{12}$ , at the null strain  $\lambda_1 = 0$  in the deformation mode are shown in Table 3 comparing with extrapolated experimental values at 0K by Kamm<sup>13</sup>. It was considered from the good agreement of both values that the model potential and the calculating process used in the present study were sufficiently reasonable. Suzuki<sup>14</sup> and Sarkar<sup>15</sup> reported other pseudopotential calculations of the elastic constants of aluminum, in which the potential parameters were determined so as to satisfy experimental values of some elastic constants, the cohesive energy, etc. in a unifying manner. The obtained values of the elastic constants are  $C_{11} = 98.8 \sim 116.7$  GPa and  $C_{12} = 78.4 \sim 88.3$  GPa by the former author, and  $C_{11} = 88.2 \sim 97.8$  GPa and  $C_{12} = 52.4 \sim 60.3$  GPa by the latter. On the other hand, the potential parameters adopted in the present calculations (c.f. Eq.(2)) were determined by using the atomic volume at 0K and experimental data of the Fermi surface as mentioned in detail in the previous paper<sup>16</sup>.

The strain dependence of  $E$  and  $\nu$  in the loading mode is shown in Fig.5. Of course,  $E$  and  $\nu$  at the point of  $\lambda_1 = 0$  are the same with the reduced values shown in Table 3.  $C_{11}$  denoted in the figure is a longitudinal elastic constant under the monoaxial strain-condition at the point of  $\lambda$  in the loading mode. Young's modulus  $E$  increases with the strain up to  $\lambda = 0.1$ , and shows its maximum there. It is considered that this feature is caused by the elastic instability on the compression side as discussed in the last section. Poisson's ratio  $\nu$  decreases with an increase of the

Table 3. Calculated and experimental values of the elastic constants  $C_{11}$  and  $C_{12}$  ( $E$  and  $\nu$  are reduced values).

	$C_{11}$ (GPa)	$C_{12}$ (GPa)	$E$ (GPa)	$\nu$
Present Calc.	111.6	62.4	66.8	0.36
Kamm's Exp.	114.30	61.92	70.78	0.351

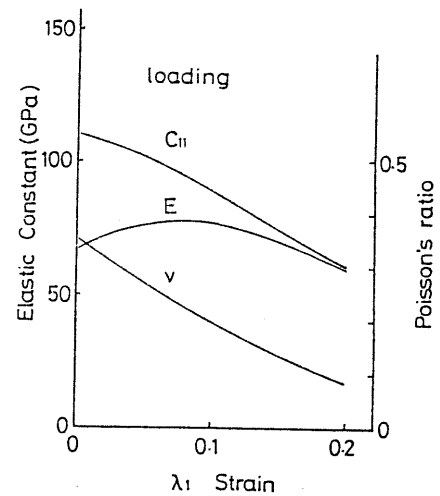


Fig.5. Variations of the elastic constants with strain in the loading mode.

stretch, and two kinds of elastic moduli,  $C_{11}$  and  $E$ , become close to each other. In the compressive deformation the values of the elastic constants were not accurately obtained because of the divergence of the derivative in energy near  $\lambda = -0.1$ . Further theoretical investigation in this field may be necessary.

### 4. Conclusions

Using the model potential proposed by the authors previously, the crystal energy of the aluminum has been evaluated as a function of the monoaxial deformations. The following conclusions are obtained.

- (1) In the compressive deformation of the (100)-loading mode, there is an elastic instability accompanied with the fcc-bcc structure-transformation. And also in the tensile deformation it is likely that a bifurcation of the deformation mode takes place as pointed out by Milstein.
- (2) In the loading mode the ideal fracture strength and fracture strain are 19.0 GPa and 0.45, respectively, where the stress-strain relation is approximately represented within 5% errors by a sine curve.
- (3) The values of the elastic constants at temperature of 0K,  $C_{11} = 111.6$  GPa,  $C_{12} = 62.4$  GPa,  $E = 66.8$  GPa and  $\nu = 0.36$ , were obtained, which are in good agreement with the experimental data. It is considered that the present calculation is a fundamental step to the further investigations of the elastic constants under various environments and conditions.

### Acknowledgements

The authors would like to express their sincere thanks to Professor Toru Nishimura

at Meijou University and Professor Nozomu Kawai at Nagoya University for their encouragements and helpful suggestions on this work, and also to Mr. Akihito Matsumuro for his assistance in the calculations. The calculations were carried out by FACOM M-200 computer system of Nagoya University Computation Center.

#### References

- (1) For example, "Elastic Constants of Metallic Materials" ed. by Jpn. Soc. Mech. Eng. (1980), 10.
- (2) Milstein, F. (ed. by Hopkins, H. G. ), "Mechanics of Solid", (1982), 417, Pergamon Press.
- (3) Milstein, F., J. Appl. Phys., 44-9(1973) 3825, 3833.
- (4) Harrison, W. A. , "Pseudopotentials in the Theory of Metals", (1966), 1, Benjamin Inc.
- (5) Heine, V. and Weaire, D. (ed. by Ehrenreich, H. ), "Solid State Physics", 24 (1970), 249, Academic Press.
- (6) Senoo, M. , et al, J. Phys. Soc. Jpn., 41-5(1976), 1562.
- (7) Fujishiro, I. , et al, Bull. JSME, 27-223(1984), 124.
- (8) Nozieres, P. and Pines, D. , Phys. Rev., 111(1958), 442.
- (9) Sham, L. , Proc. R. Soc. , Ser. A, 283 (1965), 33.
- (10) Sholl, C. A. , Proc. Phys. Soc., 92 (1967), 434.
- (11) Milstein, F. and Farber, B. , Philos. Mag. , A42-1(1980), 19.
- (12) Esposito, E. , et al, Philos. Mag., A41-2(1980), 251.
- (13) Kamm, G. N. and Alers, G. A. , J. Appl. Phys., 35-2(1964), 327.
- (14) Suzuki, T. , Phys. Rev., B3-12(1971), 4007.
- (15) Sarkar, S. K. and Sen, D. , J. Phys., F11(1981), 377.